

Gaussian beam (or plane wave)

The mathematical function that describes the **Gaussian beam** is a solution to the paraxial form of the **Helmholtz equation**.

Paraxial ray tracing assumes that the tangent and sin of all angles are equal to the angles themselves (**in other words, $\tan(u) = u$ and $\sin(u) = u$**). This approximation is valid for small angles, but can lead to the propagation of error as ray angles increase.

For a Gaussian beam, the complex electric field amplitude is given by

$$E(r, z) = E_0 \frac{w_0}{w(z)} \exp\left(\frac{-r^2}{w^2(z)}\right) \exp\left(-ikz - ik\frac{r^2}{2R(z)} + i\zeta(z)\right),$$

Where:

r is the radial distance from the center axis of the beam,

z is the axial distance from the beam's narrowest point (the "waist"),

i is the imaginary unit (for which $i^2 = -1$),

$k=2\omega n/\lambda$ is the wave number (in radians per meter), n = refractive index

$E_0 = |E(0,0)|$, the electric field (and phase) at the origin ($r = 0$, $z = 0$),

$w(z)$ is the radius at which the field amplitude and intensity drop to $1/e$ and $1/e^2$ of their axial values, respectively,

$w_0 = w(0)$ is the waist radius,

$R(z)$ is the radius of curvature of the beam's wavefronts at z distance, and

$\zeta(z)$ is the Gouy phase shift, an extra contribution to the phase that is seen in Gaussian beams.

Gouy Phase Shift

... is an additional phase shift occurring in the propagation of focused Gaussian beams.

Along its propagation direction, a **Gaussian beam** acquires a **phase shift** which differs from the one of a **plane wave** having the same **optical frequency**. It is actually not surprising that the phase shift of a Gaussian beam is not exactly the same as for a plane wave. A Gaussian beam can be considered as a superposition of plane waves with different propagation directions. This difference is called the *Gouy phase shift*.

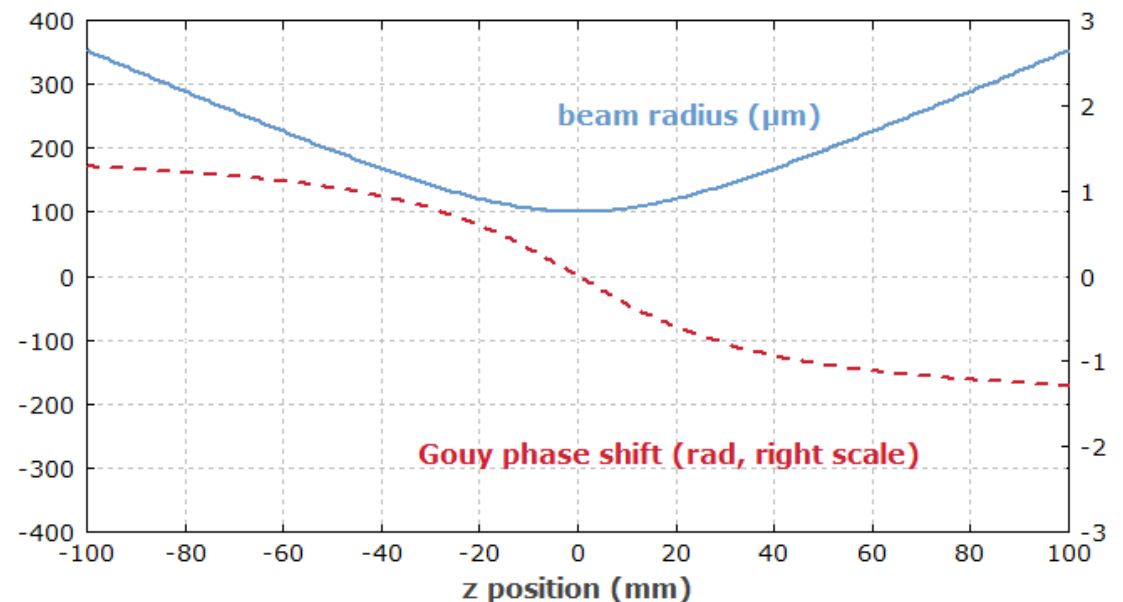
$$\varphi_G(z) = 2 \arctan \frac{z}{z_R}$$

which corresponds to a total Gouy phase shift of 2π for radially polarized light in the paraxial approximation.

z_R is the **Rayleigh length**

$z = 0$ corresponds to the position of the **beam waist**.

Beam radius and Gouy phase shift along the propagation direction for a beam in air with 1064 nm wavelength and 100 μm radius at the waist.



The Raileigh Lenght

In optics and especially laser science, the Rayleigh length or Rayleigh range, z_R , is the distance along the propagation direction of a beam from the waist to the place where the cross section area is doubled.

For a Gaussian beam propagating in free space ($n=1$) along the z axis with wave number $k = 2\pi/\lambda$ the Rayleigh length is given by

$$z_R = \frac{\pi w_0^2}{\lambda} = \frac{1}{2} k w_0^2$$

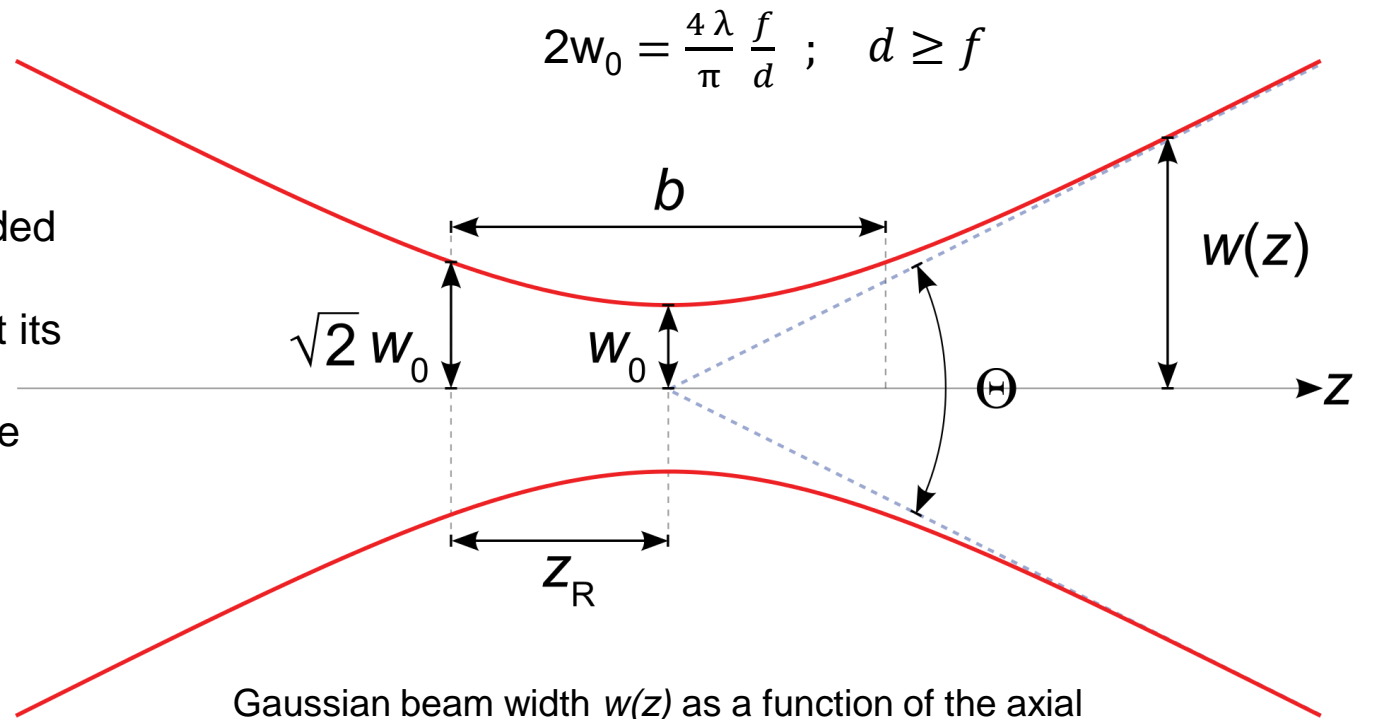
λ is the wavelength (the vacuum wavelength divided by n , the index of refraction)

w_0 is the beam waist, the radial size of the beam at its narrowest point.

This equation and those that follow assume that the waist is not extraordinarily small; $w_0 \geq 2\lambda/\pi$

The radius of the beam at a distance z from the waist is:

$$w(z) = w_0 \sqrt{1 + \left(\frac{z}{z_R}\right)^2}$$



Gaussian beam width $w(z)$ as a function of the axial distance z . w_0 : beam waist radius; b : confocal parameter; z_R : Rayleigh length; Θ : total angular spread

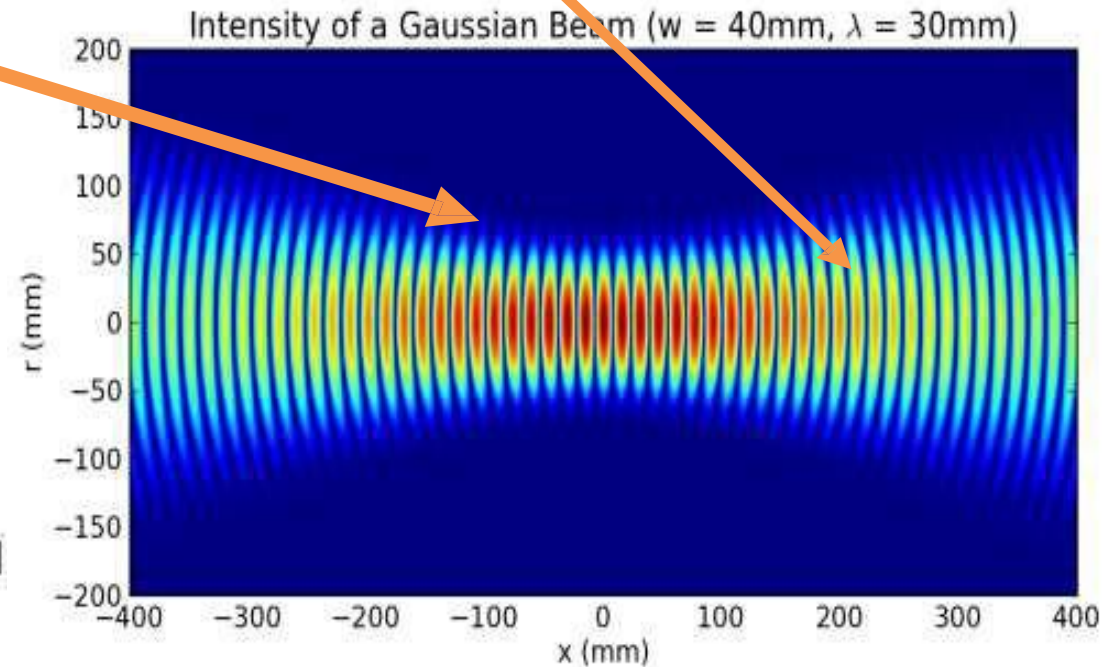
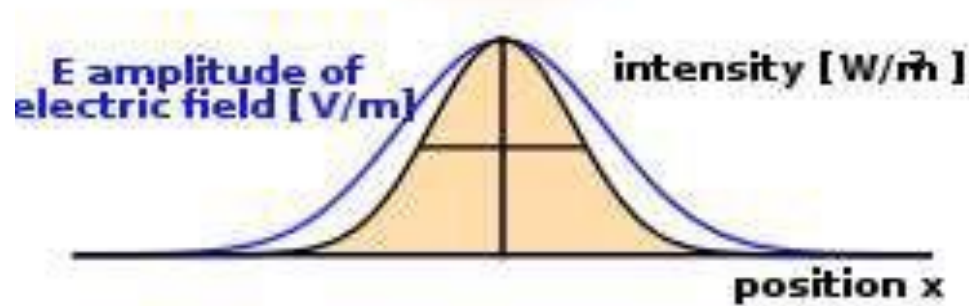
Gouy Phase Shift correction

At least theoretical is demonstrated that the domain reversal techniques of quasi-phase matching (QPM) can totally compensate for the phase error resulting from the Gouy phase shift. QPM grating designs, which are no longer linearly invariant, allow for higher efficiencies than can be obtained with standard QPM and furthermore require no shift in phase matching under focused conditions when compared to a plane wave.

* Gouy phase compensation in quasi phase matching, Huw E. Major et al., (6.08.2007)

Gaussian beam

$$E(r, z) = E_0 \frac{w_0}{w(z)} \exp\left(\frac{-r^2}{w^2(z)}\right) \exp\left(-ikz - ik\frac{r^2}{2R(z)} + i\zeta(z)\right),$$



Laser beam = "simplest"
electromagnetic field distribution

Gaussian pulse

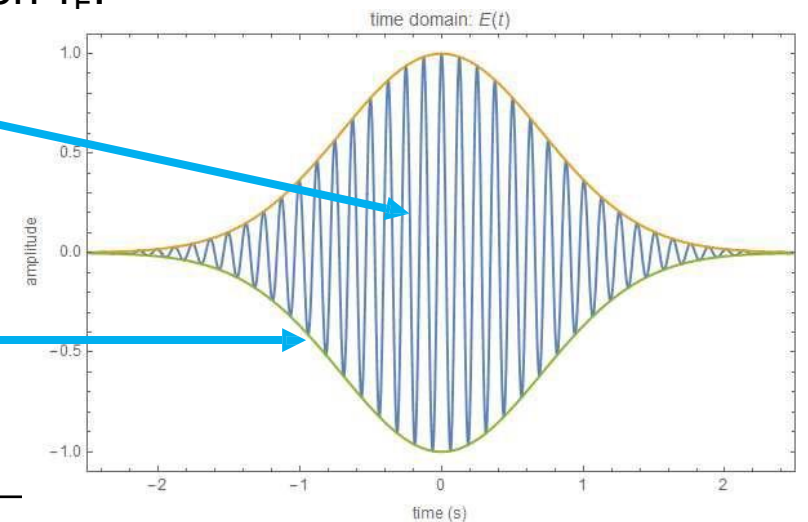
$$E(r, z) = E_0 \frac{w_0}{w(z)} \exp\left(\frac{-r^2}{w^2(z)}\right) \exp\left(-ikz - ik\frac{r^2}{2R(z)} + i\zeta(z)\right),$$

We go from cylindrical coordinates to cartesian coordinates:

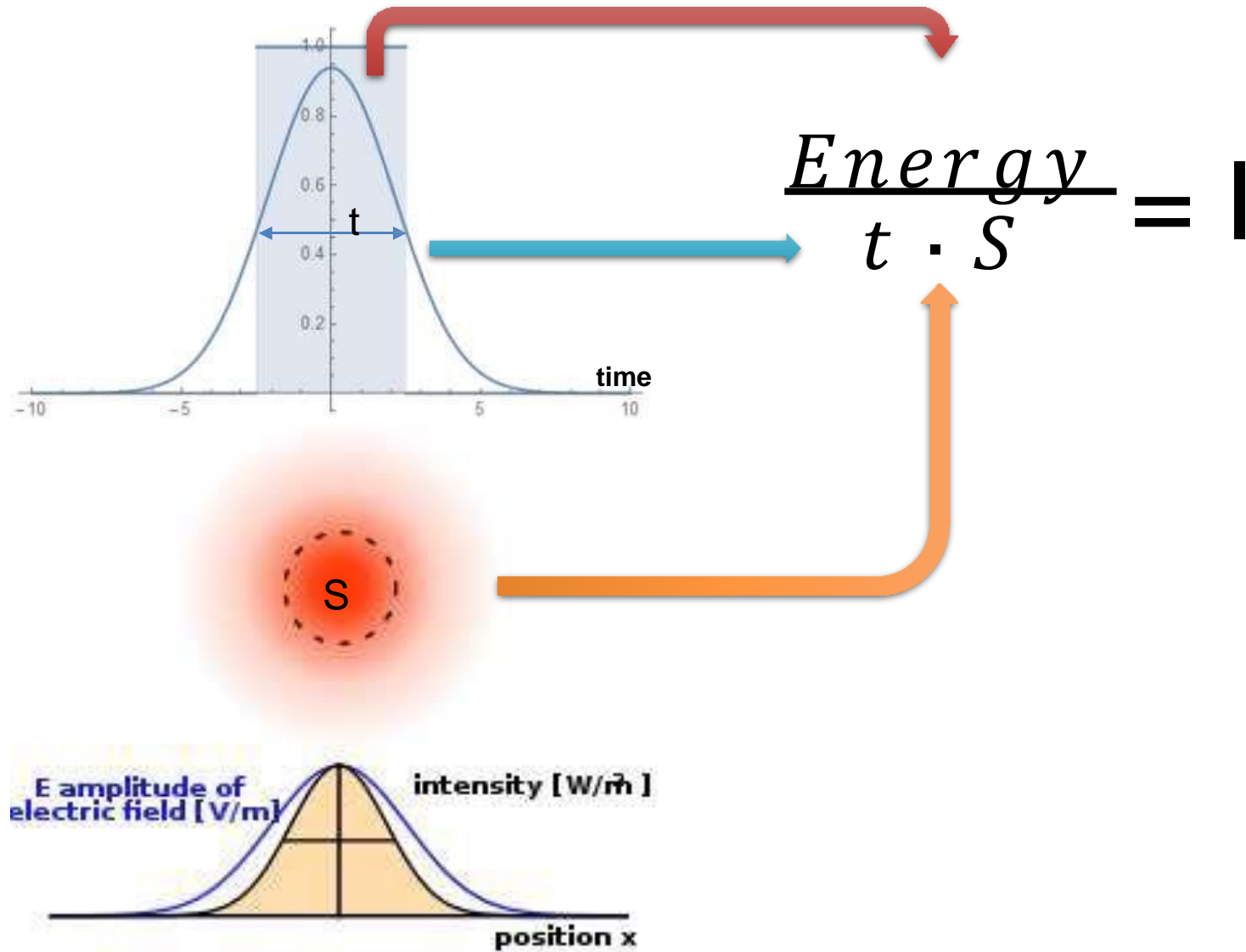
$$u(x, y, z) = u(z) \cdot \exp\left[-\frac{(x - X_0)^2 + (y - Y_0)^2}{w^2(z)}\right] \exp\left[i\frac{k}{2} \frac{(x - X_0)^2 + (y - Y_0)^2}{R(z)}\right] \cdot \exp[-i\varphi(z)] \exp(ikz).$$

We add the temporal part in the form of a Gaussian shape with duration τ_F :

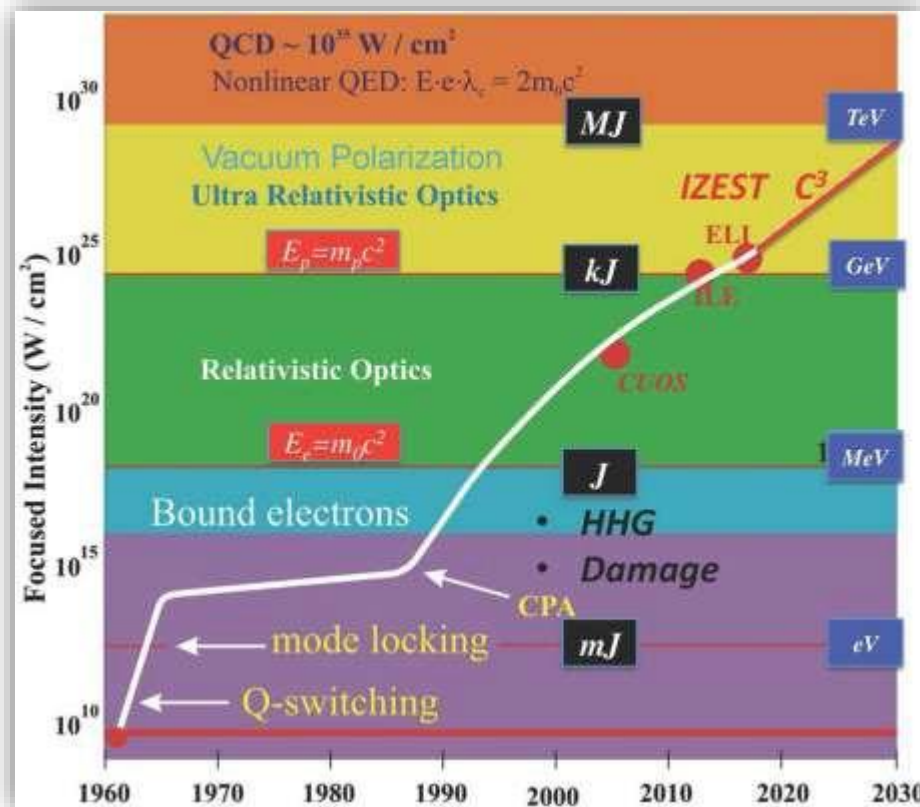
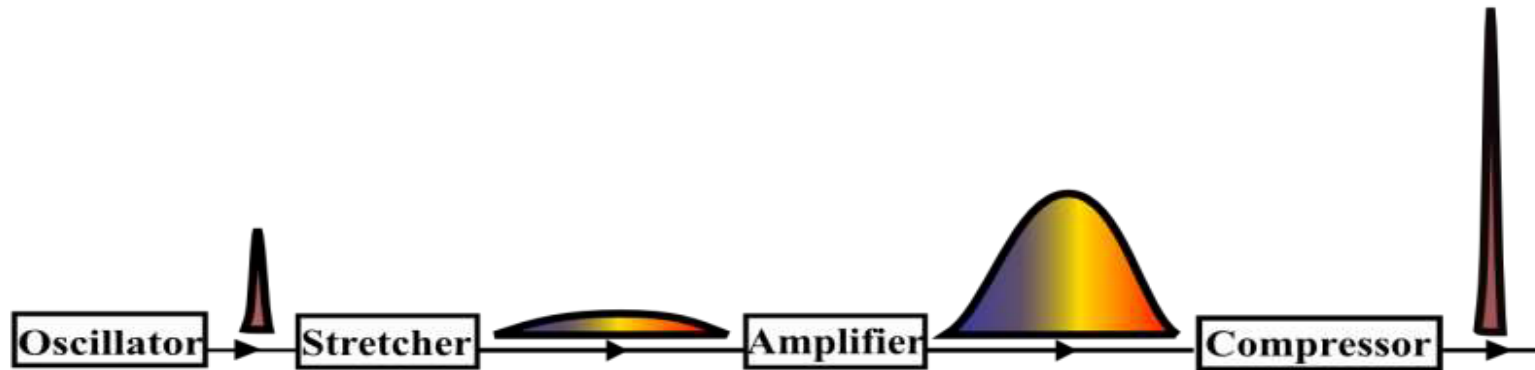
$$u(x, y, z, t) = u(x, y, z) \cdot \exp\left[-\left(\frac{z - c_0 t}{c_0 \tau_F}\right)^2\right] \cdot \exp\left[-i\frac{2\pi c_0}{\lambda} t\right]$$



Intensity

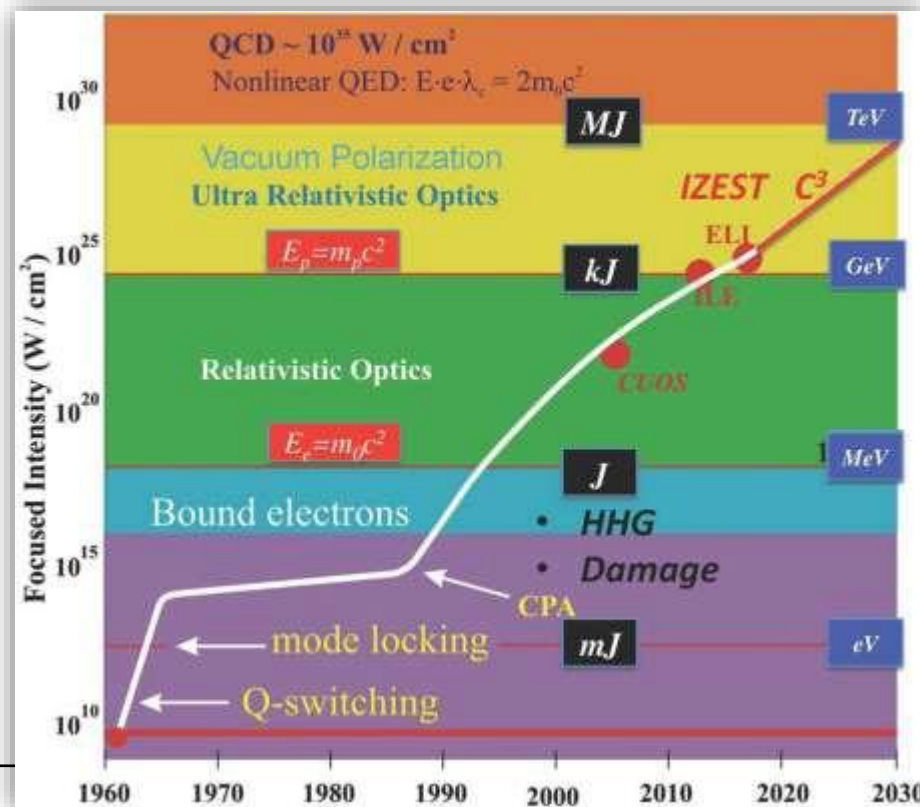
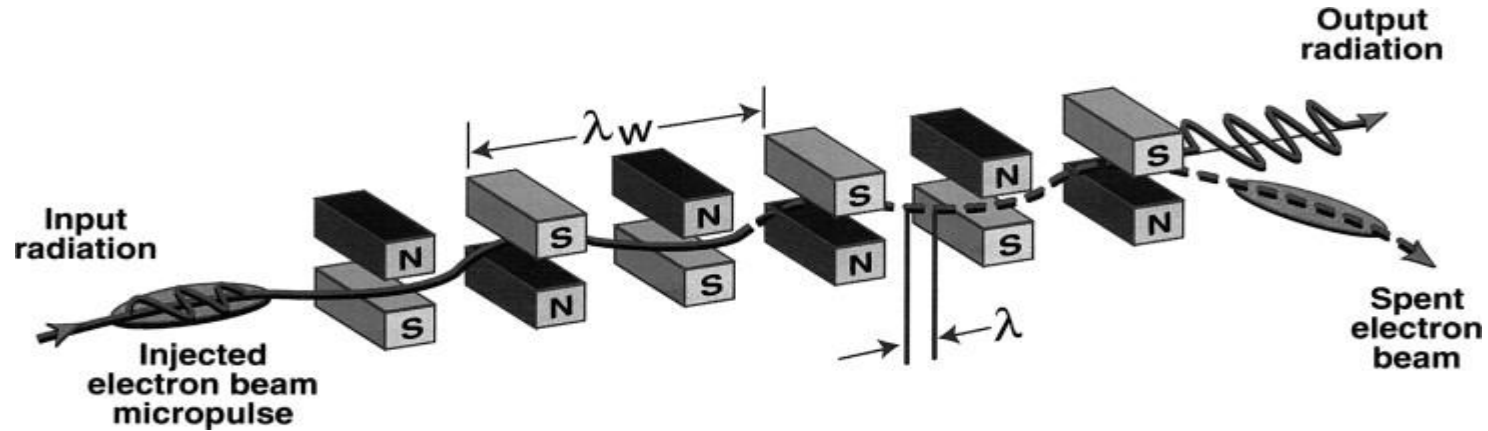


Nobel Prize 2018: Chirped Pulse Amplification



GERARD MOUROU
& DONNA STRICKLAND
(Nobel 2018)

Bound electrons

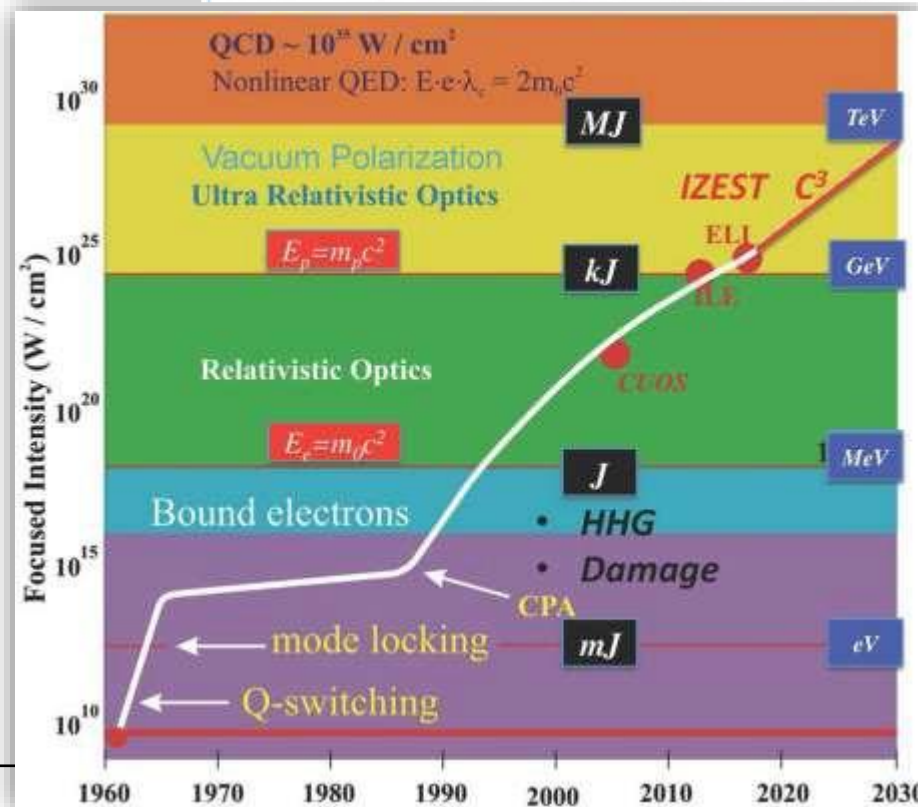
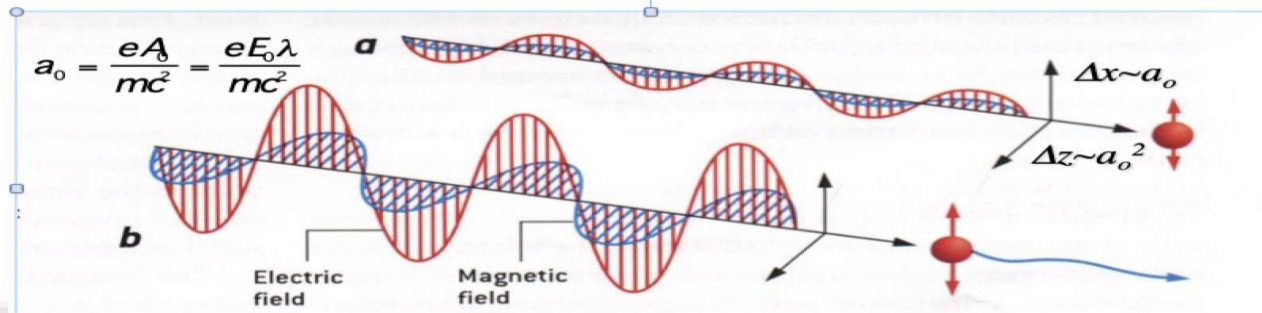


In a free-electron laser, high-energy electrons emit coherent radiation, as in a conventional laser, but the electrons travel through a vacuum instead of remaining in bound atomic states within the lasing medium. Because the electrons are free-streaming, the radiation wavelength is not constrained by a particular transition between two discrete energy levels. The radiation is produced by an interaction among three elements: the electron beam, an electromagnetic wave traveling in the same direction as the electrons, and an undulatory magnetic field produced by an assembly of magnets known as a *wiggler* or *undulator*. The wiggler magnetic field acts on the electrons in such a way that they acquire an undulatory motion. In this process, the electrons lose energy to the electromagnetic wave that is amplified and emitted by the laser.

Relativistic Optics

a) Classical optics $v \ll c$, b) Relativistic optics $v \sim c$

$a_0 \ll 1, a_0 \gg a_0^2$ $a_0 \gg 1, a_0 \ll a_0^2$



The electromagnetic field intensities produced by these techniques, in excess of 10^{18} W/cm^2 , lead to relativistic electron motion in the laser field. In contrast to the nonrelativistic regime, these laser fields are capable of moving matter more effectively, including motion in the direction of laser propagation. One of the consequences of this is plasma **wakefield** generation, a relativistic version of optical rectification, in which longitudinal field effects could be as large as the transverse ones. In addition to this, other effects may occur, including relativistic focusing, relativistic transparency, nonlinear modulation and multiple harmonic generation, and strong coupling to matter and other fields (such as high-frequency radiation). A proper utilization of these phenomena and effects leads to the new technology of relativistic engineering.

Plasma wakefield acceleration

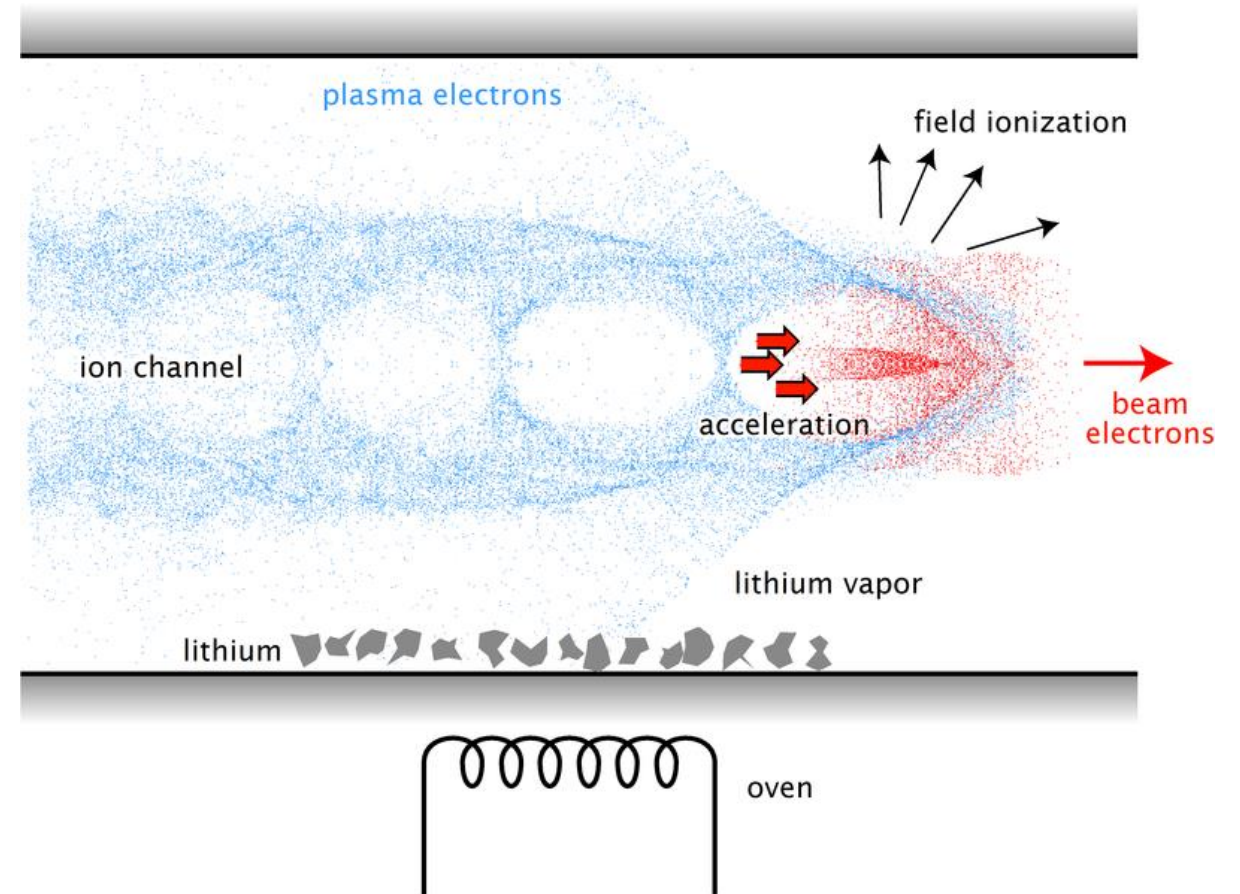
Plasma = fluid of positive and negative charged particles.

In particular: mix of electrons and ions in equilibrium.

Under a strong enough external electric or electromagnetic field, the plasma electrons, which are very light in comparison to the background ions (by a factor of 1836), will separate spatially from the massive ions creating a charge imbalance in the perturbed region.

The plasma medium acts as the most efficient transformer (currently known) of the transverse field of an electromagnetic wave into longitudinal fields of a plasma wave.

A laser pulse can be used to excite the plasma wake. As the pulse travels through the plasma, the electric field of the light separates the electrons and nucleons in the same way that an external field would.



Laser pulses parameters

- Electric field E_L (V/cm) = $2.75 \times 10^9 \left(\frac{I_L}{10^{16} \text{ W/cm}^2} \right)^{1/2}$
 - Magnetic field B_L (Gauss) = $9.2 \times 10^6 \left(\frac{I_L}{10^{16} \text{ W/cm}^2} \right)^{1/2}$
 - Pressure $P_L = \frac{I_L}{c} (1 + R) \approx 3.3 \text{ Mbar} \left(\frac{I_L}{10^{16} \text{ W/cm}^2} \right) (1 + R)$
-

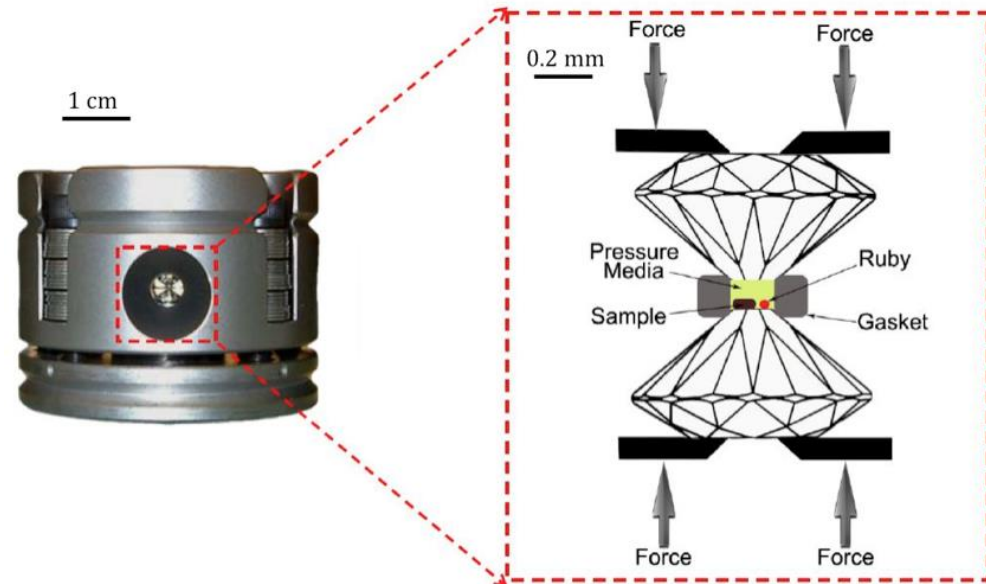
Parameter comparison

• Magnetic field

- 1 MG Strongest pulsed non-destructive magnetic field produced in a laboratory, Pulsed Field Facility at National High Magnetic Field Laboratory's, Los Alamos National Laboratory, (Los Alamos, NM, USA).
- 12 MG Record for indoor pulsed magnetic field, (University of Tokyo, 2018)
- 28 MG Record for human produced, pulsed magnetic field, (VNIIEF, 2001)
- 10 GG - 1 TG Strength of a non-magnetar neutron star.
- >9.2 GG in reach at ELI-NP

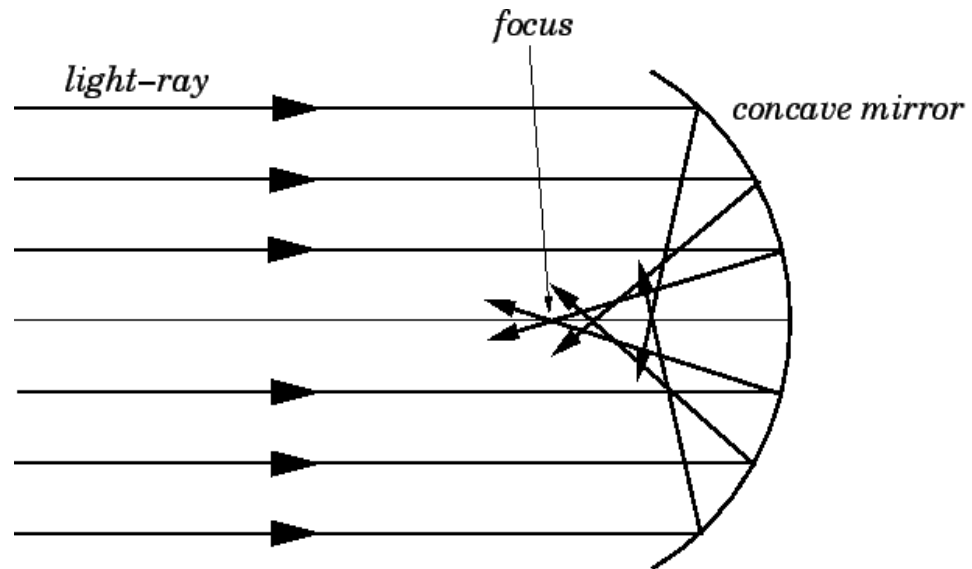
• Pressure

- >600 GPa = 6×10^6 bar: Pressure attainable with a diamond anvil cell
- 5TPa = 5×10^7 bar: Pressure generated by the National Ignition Facility fusion reactor
- 2.5×10^{11} bar Pressure inside Sun's core
- $>3.3 \times 10^{12}$ bar in reach at ELI-NP



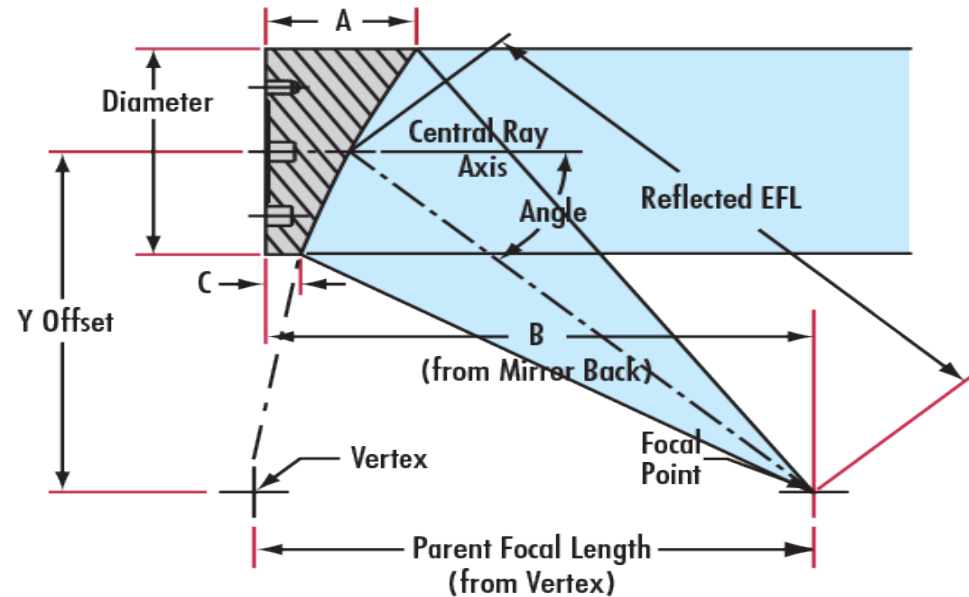
Laserul PW

Using normal mirrors (f/1), CPA technology allows intensities of maximum 2×10^{22} W/cm² for Ti:sapphire crystals.

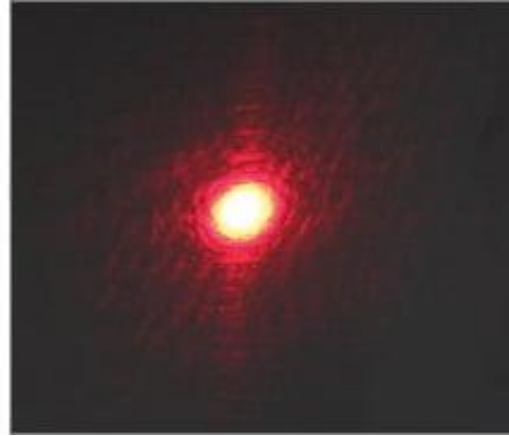


For higher powers one have to use f/3 off-axis parabolic mirrors, able to focus with minimum optical aberations.

Off-Axis Parabolic Metal Mirrors



f/3 off-axis parabola mirrors

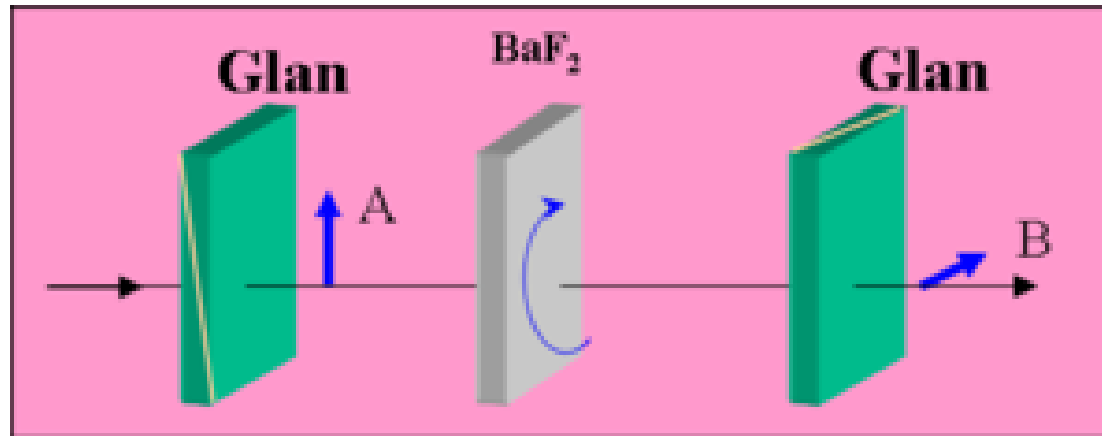


- > High energy amplification of chirped laser pulses is limited by the size of available optical components, like Ti:sapphire crystals from final amplifiers, diffraction gratings from temporal compressors and mirrors.
 - > In case of a Gaussian spectral profile with perfect phase locking of the amplified spectral components, transform-limited laser pulses can be generated after re-compression. Gain narrowing and red-shifting during Ti:sapphire amplification contribute to the increase of the amplified re-compressed pulse.
 - > In order to preserve a broad amplification bandwidth, special techniques are used in the chirped pulse amplification chains, like optical parametric chirped pulse amplification - OPCPA, cross-polarized wave generation – XPW, and spectrum management using acousto-optic programmable dispersion filters (AOPDFs).
-

Cross-polarized wave (XPW)

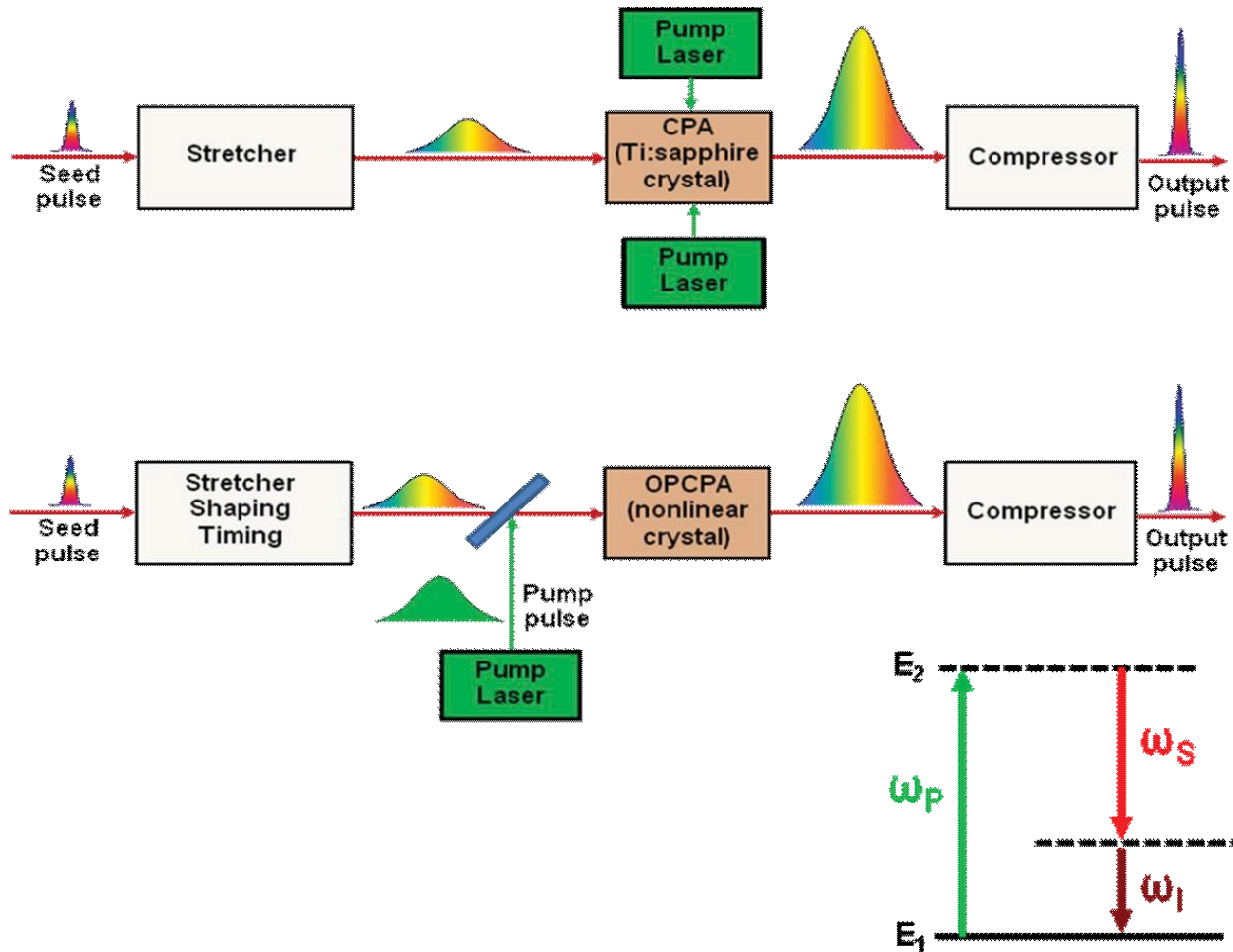
Cross polarized wave generation (XPW) is a well established technique for contrast enhancement of ultrashort pulses in high energy laser systems. XPW is a nonlinear optical process that can be classified in the group of frequency degenerate (four-wave mixing) processes. It can take place only in media with anisotropy of third-order nonlinearity. As a result of such nonlinear optical interaction, at the output of the nonlinear crystal is generated a new linearly polarized wave at the same frequency, but with polarization oriented perpendicularly to the polarization of input wave. Implementation of XPW is quite straightforward: a linearly polarized laser pulse is focused into a crystal positioned in between two crossed polarizers. Efficient conversion with XPW only occurs at high intensities.

Simplified optical scheme for XPW generation is shown on next figure. It consists of a nonlinear crystal plate (thick 1-2 mm) sandwiched between two crossed polarizers. The intensity of generated XPW has cubic dependence with respect to the intensity of the input wave. In fact this is the main reason this effect is so successful for improvement of the contrast of the temporal and spatial profiles of femtosecond pulses. Since cubic crystals are used as nonlinear media they are isotropic with respect to linear properties (there is no birefringence) and because of that the **phase** and **group velocities** of both waves XPW and the fundamental wave (FW) are equal: $Ph_{XPW}=Ph_{FW}$ and $V_{gr,XPW}=V_{gr,FW}$. Consequence of that is ideal phase and group velocity matching for the two waves propagating along the crystal. This property allows obtaining very good efficiency of the XPW generation process with minimum distortions of the pulse shape and the spectrum.



CPA versus OPCPA

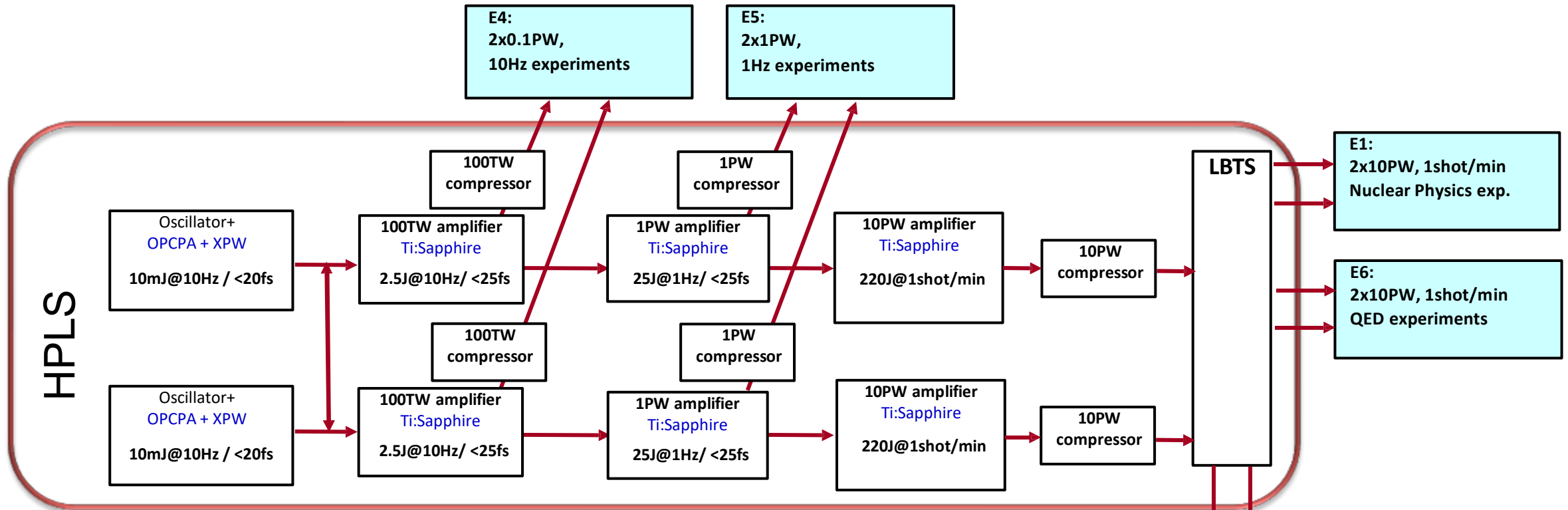
The principle of CPA in laser active media (e.g. Ti:sapphire crystals suitable for large spectral bandwidth CPA) and the principle of OPCPA in nonlinear crystals are presented in the next figure.



Due to the depletion of the upper laser level population, in the amplifiers working near the saturation regime, the amplification of the “red” spectral components coming in the leading edge of the laser pulse is significantly higher than for the “blue” spectral components arriving on the trailing edge of the pulse. The result is a red shift of the output spectrum accompanied by spectrum narrowing too. Due to the spontaneous emission amplification, which takes place as long as stored energy in the upper laser level exists, the intensity contrast of amplified femtosecond pulses decreases. Transversal lasing in the large size Ti:sapphire amplifiers limits the high energy pumping and high pulse energy amplification.

In case of parametric amplification, the energy is not stored in the nonlinear crystal. Amplification takes place only when seed pulse and pump pulse are spatially and temporally overlapped in the nonlinear crystal. In the first step, by absorption of pump photons with ω_p frequency, the crystal molecules leave from their ground energy level E_1 to an intermediate energy level E_2 . In the second step, while a molecule returns to its initial state, a photon with ω_s frequency of the seed photons and one “idler” photon with $\omega_i = \omega_p - \omega_s$ are simultaneously created. This process is practically instantaneous compared to the seed and pump pulse duration. The parametric amplification is produced under conditions of photons energy conservation and phase matching, for a certain orientation of the crystal.

The High Power Laser System at ELI-NP (HPLS)



Measured parameters of the HPLS

Output type	100 TW	1 PW	10 PW
Pulse energy (J) *	2.7	25	242
Pulse duration (fs) **	< 25	< 24	<23
Repetition rate (Hz)	10	1	1/60
Calculated Strehl ratio from measured wavefront	> 0.9	> 0.9	> 0.9
Pointing stability (μrad RMS)	< 3.4	< 1.78	< 1.27
Pulse energy stability (rms)	< 2.6 %	< 1.8 %	< 1.8 %

*Calculated considering the transmission efficiency of temporal compressors

**Measured with attenuated input energy in the compressors

E1:
2x10PW, 1shot/min
Nuclear Physics exp.

E6:
2x10PW, 1shot/min
QED experiments

40m

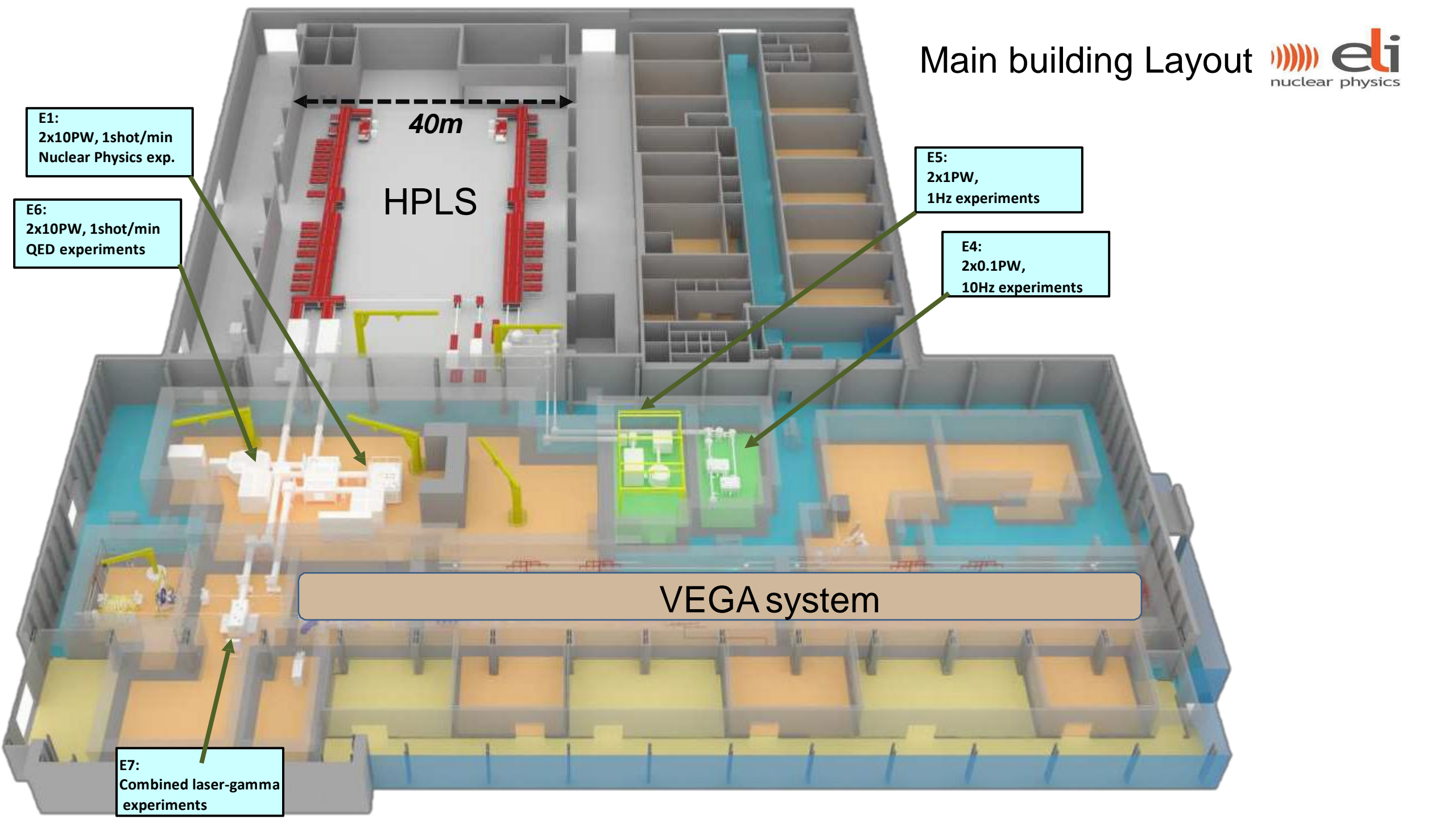
HPLS

E5:
2x1PW,
1Hz experiments

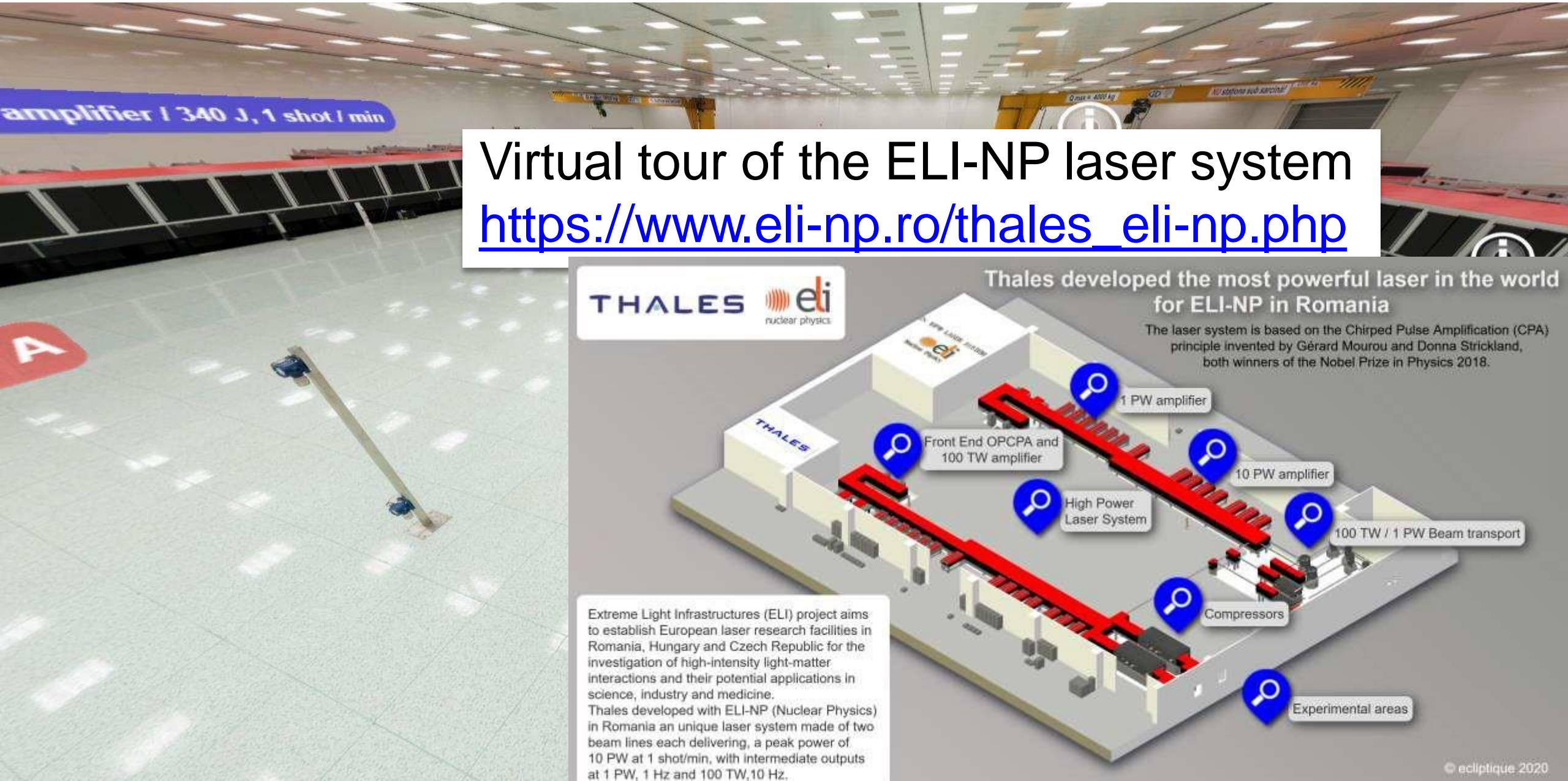
E4:
2x0.1PW,
10Hz experiments

VEGA system

E7:
Combined laser-gamma
experiments



The High Power Laser System at ELI-NP (HPLS)

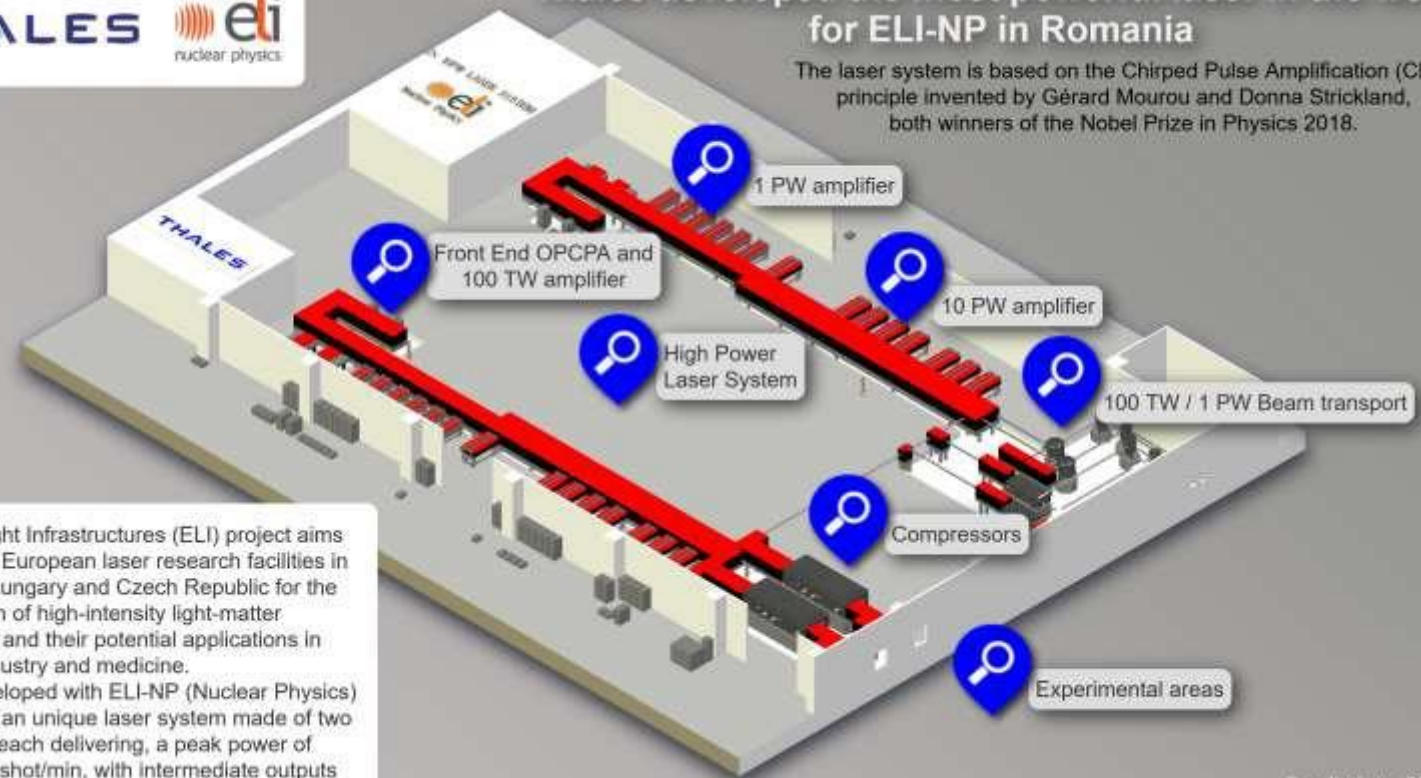


Virtual tour of the ELI-NP laser system
https://www.eli-np.ro/thales_eli-np.php



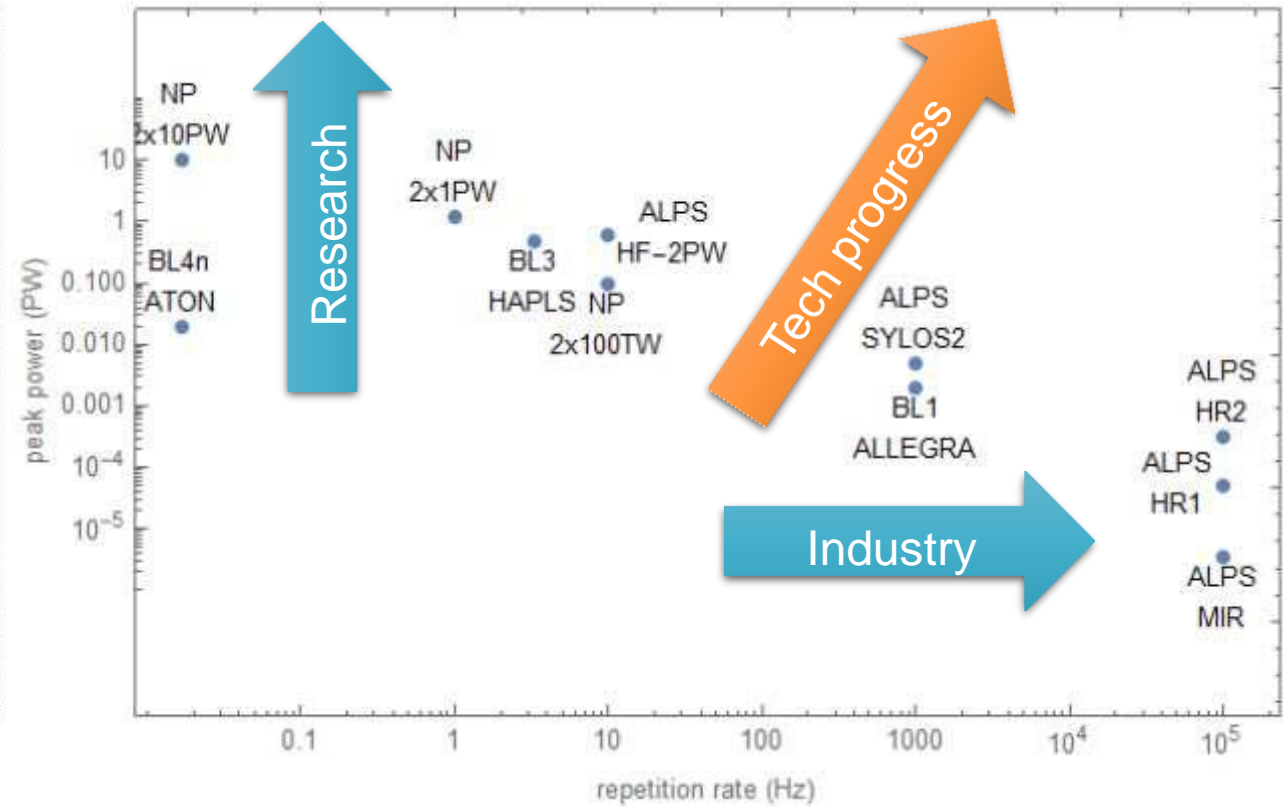
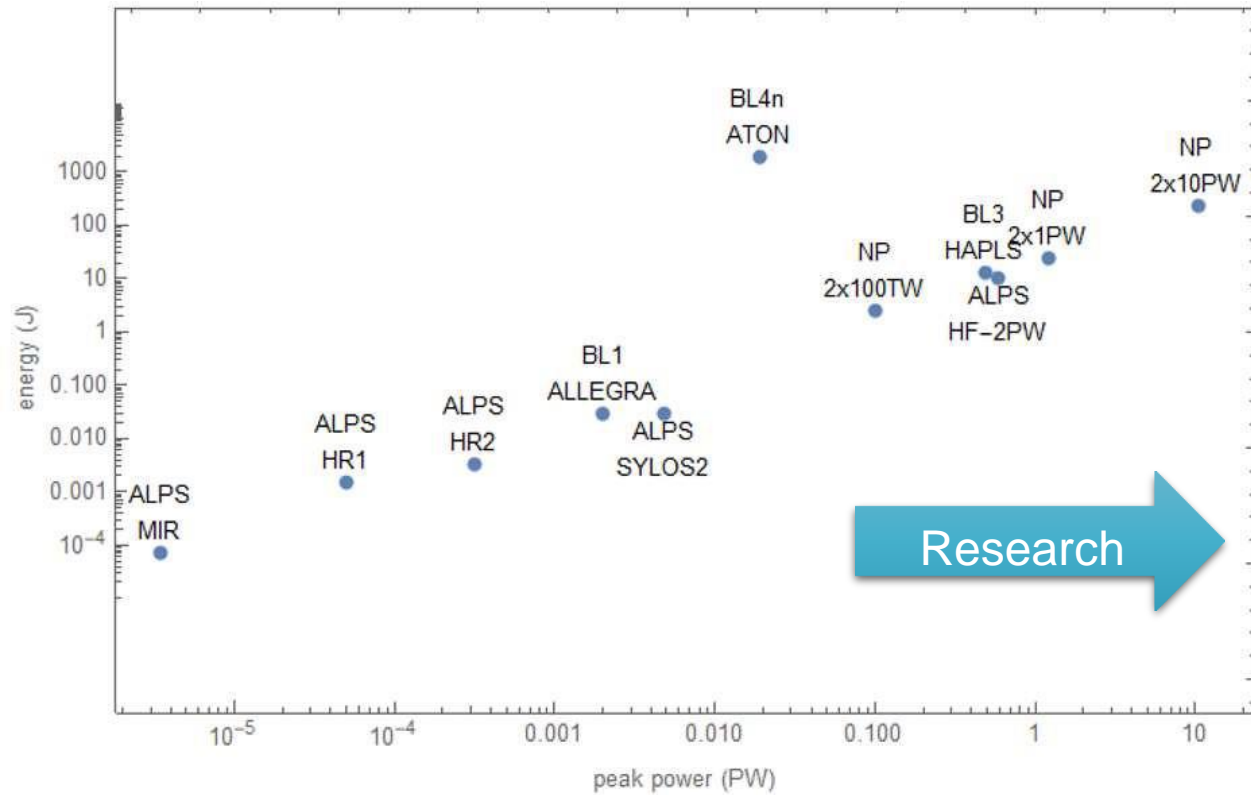
Thales developed the most powerful laser in the world for ELI-NP in Romania

The laser system is based on the Chirped Pulse Amplification (CPA) principle invented by Gérard Mourou and Donna Strickland, both winners of the Nobel Prize in Physics 2018.

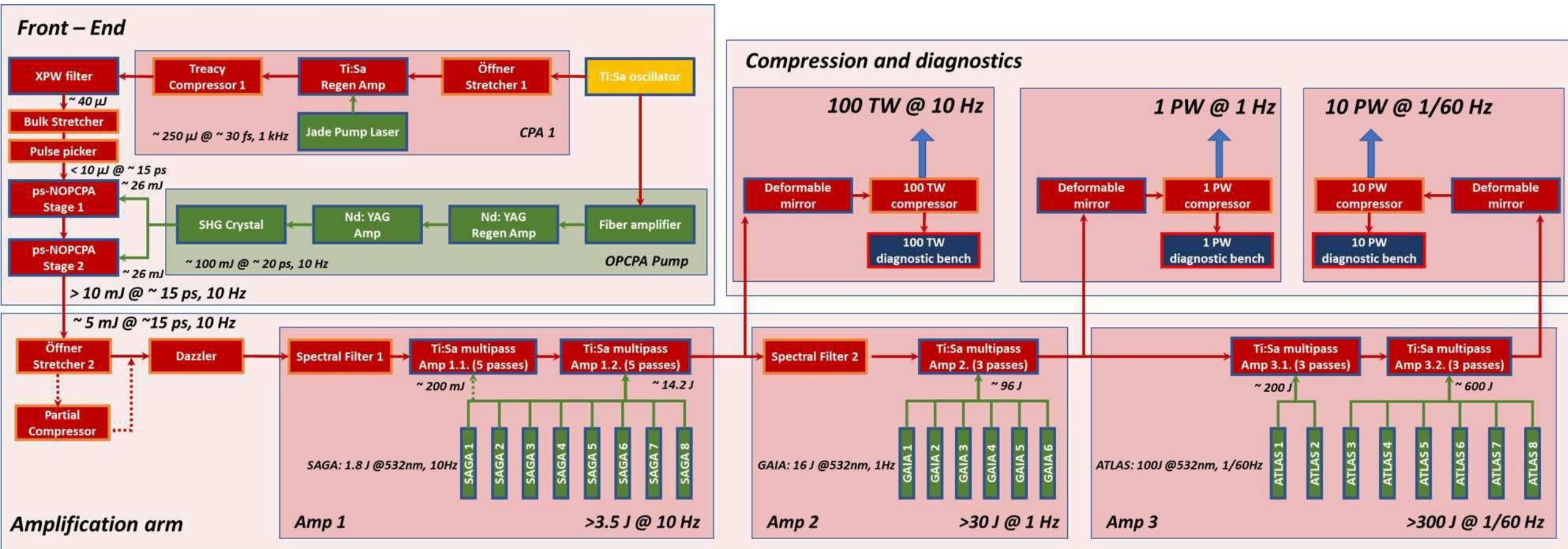


Extreme Light Infrastructures (ELI) project aims to establish European laser research facilities in Romania, Hungary and Czech Republic for the investigation of high-intensity light-matter interactions and their potential applications in science, industry and medicine. Thales developed with ELI-NP (Nuclear Physics) in Romania an unique laser system made of two beam lines each delivering, a peak power of 10 PW at 1 shot/min, with intermediate outputs at 1 PW, 1 Hz and 100 TW, 10 Hz.

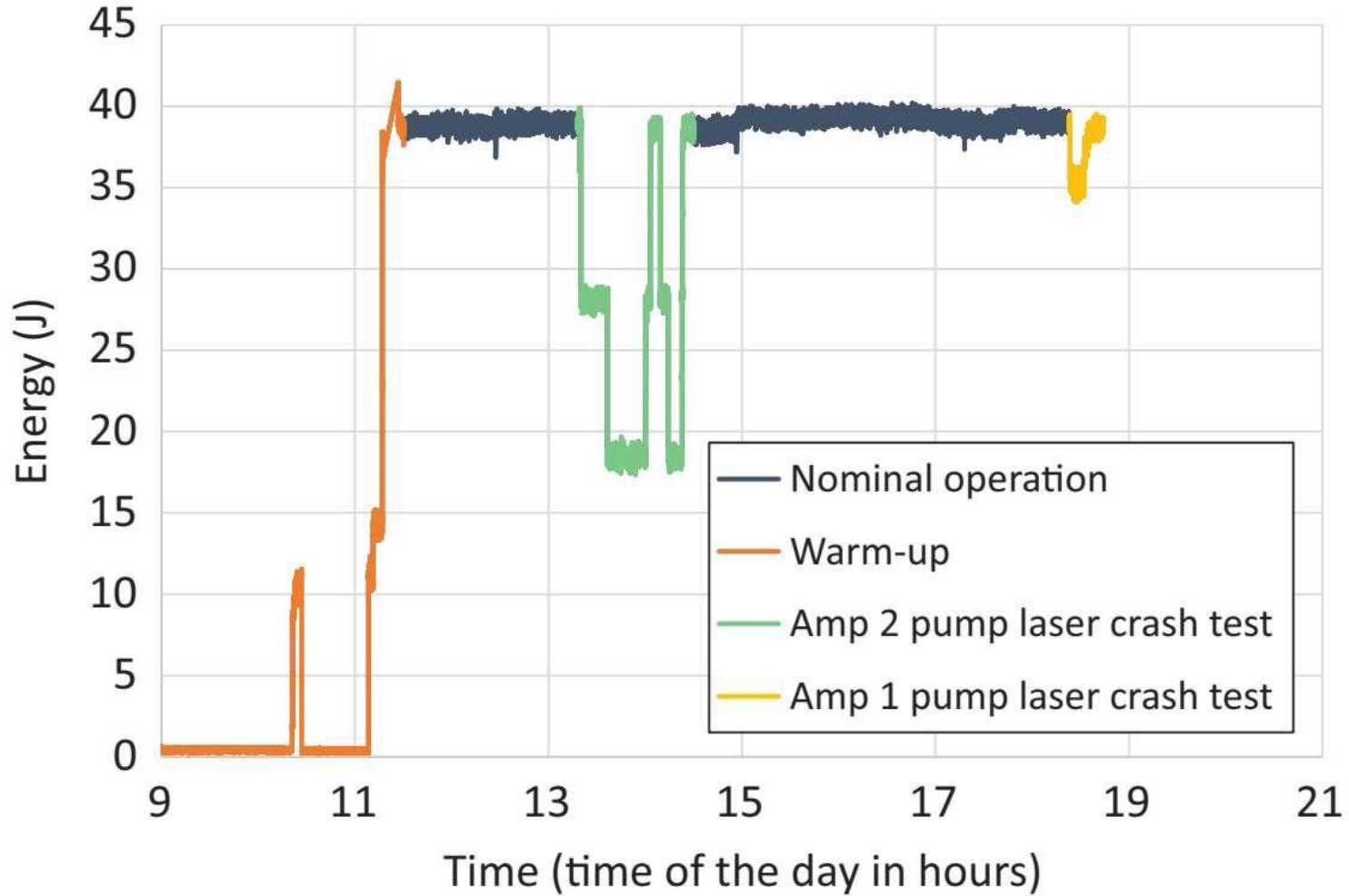
ELI performance - end of 2020



HPLS layout



Energy stability for Amplifier 2



≥25000 shots/day